

# Microsized 3D Hydrogel Printing System using Microfluidic Maskless Lithography and Single Axis Stepper Motor

Jinsik Yoon & Wook Park \*

Received: 25 June, 2020 / Accepted: 26 July, 2020 / Published online: 11 September, 2020  
©The Korean BioChip Society and Springer 2020

**Abstract** The 3D printing apparatus in conventional inkjet and stereolithography systems is limited to continuous fabrication of a microsized three-dimensional hydrogel composed of multiple substances. We present a micro three-dimensional printing system by combining a polydimethylsiloxane microfluidic channel through which various fluids can flow into a micro two-dimensional particle generation system, and a single-axis stepper motor to control the thickness of each layer. The optimal channel designs for micro three-dimensional printing were set up through a physics simulation program and using the simulation analysis, the optimal microfluidic channel was fabricated. Through the system and channel, three-dimensional micropatterns and particles could be fabricated and the generated microparticles automatically collected by the washing flow in the channel. Zinc oxide nanoparticle materials transparent, biocompatible, and capable of absorbing ultraviolet light were added to the premixed photocurable solution used for the microparticle production, and thereby precise micro three-dimensional patterns and particles could be fabricated. In addition, by transporting a variety of fluids into the microfluidic channel, it was possible to create micro three-dimensional particles composed of heterogeneous materials.

**Keywords:** 3D printing, Multimaterial, Microfluidics, Microfabrication, Hydrogel

Department of Electronics and Information Convergence Engineering,  
Institute for Wearable Convergence Electronics, Kyung Hee University,  
1732, Deogyongdaero, Giheung, Yongin 17104, Republic of Korea

\*Correspondence and requests for materials should be addressed to  
W. Park (✉ parkwook@khu.ac.kr)

## Introduction

Microfabrication process technology has helped in the development of microchip systems such as integrated circuits<sup>1–3</sup> and microfluidic channel devices<sup>4–7</sup>. In particular, microfluidic devices have been used where various microstructures or particles are fabricated using flow-focusing and photolithography systems. In the flow-focusing method<sup>8–10</sup>, spherical microparticles can be produced in large quantities, and special microparticles containing various prepolymer can be produced by flowing heterogeneous materials<sup>11,12</sup>. The photolithography technique is a method for mass production of various desired two-dimensional microparticles or patterns, and it is used in a variety of fields such as micropatterning<sup>13,14</sup> and anti-counterfeiting<sup>15</sup>. It has also been applied to microfluidic technology and complicated two-dimensional pattern production using various substances<sup>16–21</sup>. Despite all these studies, demands for more diverse and complex structures have increased, and, simultaneously, the interest in three-dimensional microfabrication has risen. In order to construct simple three-dimensional microstructures, the photolithography method using light spread according to environmental factors has been used<sup>22–25</sup>. To create more exquisite and intricate three-dimensional microstructures, inkjet three-dimensional printing technology<sup>26–28</sup> has been introduced; multiphoton-based methods<sup>29–32</sup> have also been utilized in various fields. However, these methods have limitations of resolution based on nozzle size and multimaterial application. Therefore, the demands of various three-dimensional microstructure fabrication systems that have easy resolution adjustment and use multiple materials have increased.

In this study, we propose a versatile method for fabricating a three-dimensional micropattern, particle, and structure using a two-dimensional micropattern and particle generation system—optofluidic maskless lithography (OFML)—with a microfluidic chip made up of polydimethylsiloxane (PDMS) and a single-axis stepper motor to facilitate height adjustment. The washing solution is flowed into the microfluidic channel to initialize production, and it is possible to automatically collect fabricated three-dimensional microparticles and structures. Based on the simulation results, the optimal microfluidic channel design according to the height of the structure to be fabricated was obtained, and the designed channel applied to the three-dimensional printing system. Furthermore, considering delicate thickness adjustment and potential applicability in biomedical fields, particular materials were mixed with a photopolymer to control the depth which light can penetrate, and three-dimensional microstructures consisting of various materials fabricated by transporting solutions of different components into the microfluidic channel.

## Results and Discussion

### Micro 3D Hydrogel Printing System using Microfluidic Maskless Lithography System and Single-Axis Stepper Motor

In order to fabricate three-dimensional polymeric microparticles, an OFML system that can synthesize two-dimensional micropatterns and particles from photopolymerization of photocurable resins in a microfluidic channel by modulating a digital micromirror device (DMD) capable of reflecting light of desired shapes to a specific direction by switching the dynamic mirrors, and a minutely controllable single-axis stepper motor were used. They are shown in Figure 1.

The OFML system is very similar to the stereolithography technique used in 3D printing, if additional equipment that can regulate height of the microfluidic channel is added. Therefore, a single-axis stepper motor was adapted to the OFML system in order to press and release the membrane of the microfluidic channel to formulate three-dimensional micropatterns and particles.

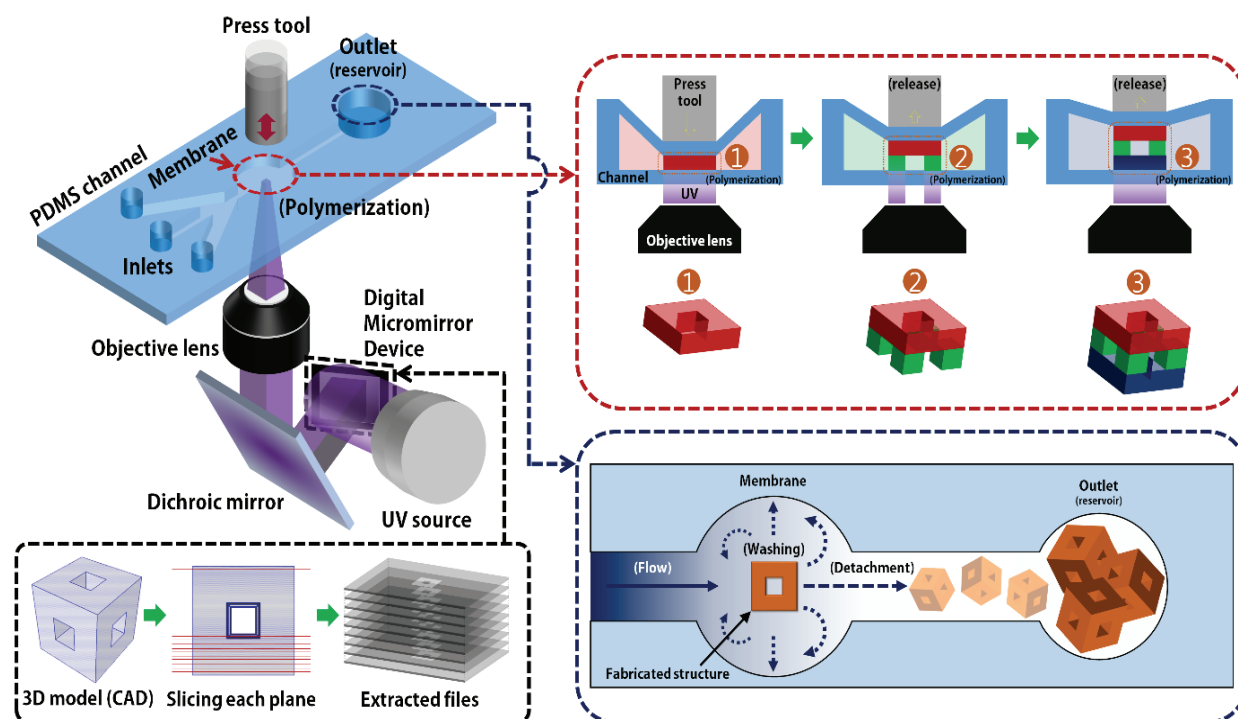


**Figure 1.** Schematic illustration of a micro three-dimensional printing system. The system consists of microfluidic maskless photolithography system to consecutively project dynamic light patterns, and a single-axis stepper motor for adjusting PDMS channel height. By using sequentially-exchanging resin materials on the microfluidic channel, various 3D structures composed of multiple materials can be created. Also, fabricated microstructures can be automatically washed and collected to the outlet, the reservoir, by detaching particles using the flow of the fluid.

The procedure for generating the three-dimensional micropatterns and particles is as follows: First, to create a three-dimensional object, a 3D drawing (computer-aided design, CAD) file was loaded into an image processing tool such as MATLAB program, and the object sliced to a desired thickness and stored as sequential image files to input the cross-sectional shape into the DMD of the OFML system. Second, through microfluidic channel inlets, the solution to be used in the production was transported into the channel, and the thickness of the layer to be fabricated adjusted by controlling the single-axis stepper motor. Third, in order to fabricate the desired three-dimensional object using photopolymerization, the patterned light to be irradiated into the channel was controlled by the DMD and a single layer created. The patterned light was adjusted by inserting the image files that were prepared in the first step into the DMD on which bmp or jpg format extension files with a single bit or grayscale image representation could be loaded. Fourth, to additionally build the next layer, the single-axis stepper motor was moved up to the next layer thickness to secure the fabrication space, and the light was irradiated in order to create the next layer. By repeating these processes, three-dimension-

nal micropatterns and particles could be produced. In addition, by flowing a variety of materials to be formed in each layer through the multiple inlets, multi-material three-dimensional micropatterns and particles which can be made of various materials for each layer could be fabricated. At the end of production, the washing solution was adequately flowed to detach the object, and the fully-created structure could be automatically collected to the outlet.

### Optimized Microfluidic 3D Printing Channel Design

To maximize the use of limited resources, generating the microstructures using a minimum volume of solutions is important. Therefore, in this experiment, we determined the maximum height of the structures that can be created according to the design of the microfluidic channel in a microfluidic 3D printing system. Before fabricating the microfluidic channel, a simulation was performed using COMSOL Multiphysics program to obtain the protractile vertical length of the channel cover according to the channel design as shown in Figure 2.

The microfluidic channel was made from PDMS

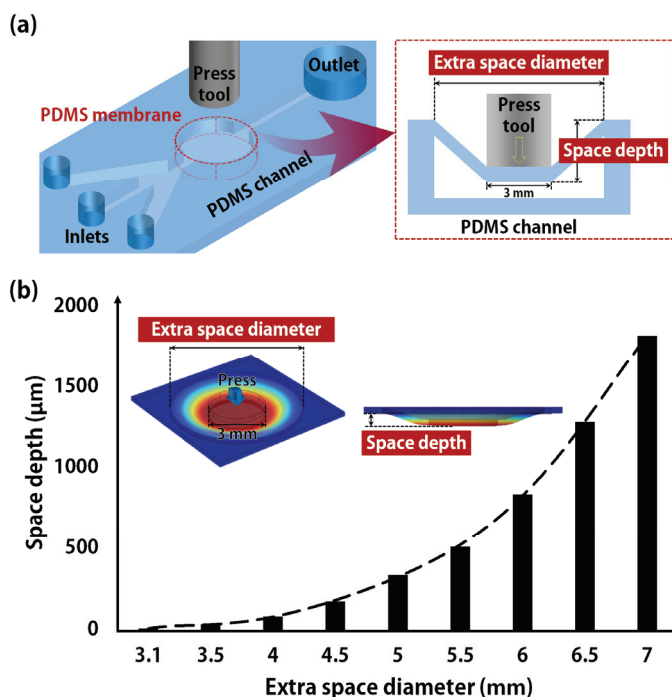


**Figure 2.** Simulation of the optimized microfluidic channel design used on the 3D printing system to ascertain limited conditions of three-dimensional objects that can be created. (a) Illustration of the microfluidic-based 3D printing channel and cross section of the PDMS membrane area (external force pressing section with a diameter of 3 mm and a circular extra space). (b) The simulation results of the calculated space depth of the three-dimensional microstructure printing channel against extra space diameters. The values of the results show limited maximum height of the microstructure according to the channel design with extra space size.

(Sylgard 184, Dow Corning), and the upper part, i.e., cover of the channel, made of an equal PDMS sheet with a thickness of 250  $\mu\text{m}$  that was chemically bonded to the channel through air plasma treatment process. In addition, since the fabricated micropatterns and particles must be adhered to the microfluidic channel cover part, a circular thin glass slide (microscope slide, 1mm thickness, DURAN), cut manually by a glass cutter and abrasive disc with diameter of 3 mm, was bonded through the plasma process to the bottom of the thin cover inside of the channel. In order to symmetrically balance the stress of the cover part when an external force is applied, both the inner space of the channel and the pressing part of the single-axis stepper motor are designed to be isotropic, and circular in shape.

We assumed that the center portion of the channel cover, within a 3-mm diameter, to be pressed by an external force and no longer stretched because the 3-mm diameter glass slide was bonded to the bottom of the channel cover and the pressing part of the single-axis stepper motor had an equal size. Also, the external force applied to the channel cover part, PDMS modulus, and Poisson's ratio were set to 0.1 N, 0.93

MPa, and 0.4999, respectively.

As a result of the simulation, we were able to predict the maximum height of micropatterns and particles that could be fabricated according to the extra space diameter in the microchannel design, and this is shown in Figure 2(b). If the extra space diameter was large, it would be feasible to create higher microstructures, but large amounts of solution volume would be consumed. Therefore, based on the simulation results, after selecting the micropattern and particle size and height to be fabricated, we could design the optimal microchannel with minimal waste.

### Fabrication of Three-Dimensional Microstructure with High Resolution

By utilizing the microfluidic three-dimensional printing system and adopting the designed extra space diameter of 4.5 mm microfluidic channel from the simulation results above, we could fabricate the 3D microstructures shown in Figure 3. In order to create the microparticles and patterns, a premixed photocurable solution, polyethylene glycol diacrylate (PEGDA, Mn = 700, Sigma-Aldrich) mixed with 10% v/v 2-hy

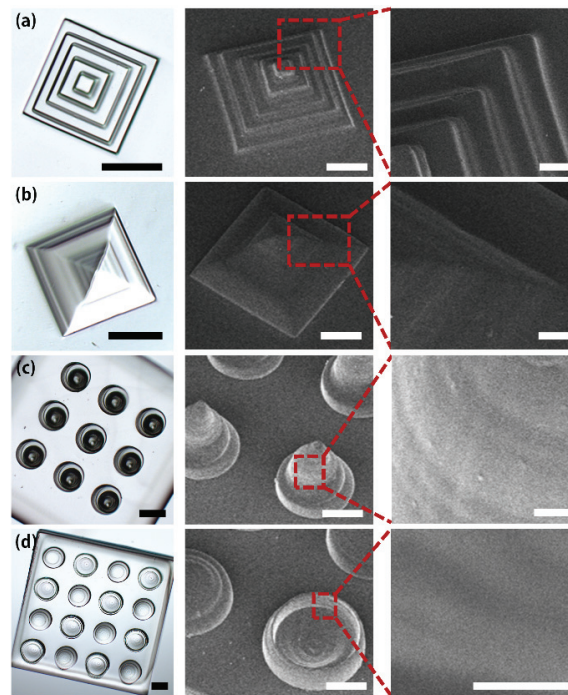


**Figure 3.** Fabricated three-dimensional microstructures created by utilizing a three-dimensional printing system with a microfluidic channel. (a) 5-layer pyramid, (b) 51-layer pyramid, (c) microneedle, and (d) microlens structures were created on each layer: (a) 34-micrometer and (b,c,d) 3.4-micrometer-thick layers, respectively. The left images were observed by optical microscope, and the center and right images by SEM. Also, the right images show details of the center photographs. (Scale bars: 200  $\mu\text{m}$  (left), 100  $\mu\text{m}$  (center), 20  $\mu\text{m}$  (right, (a) and (b)), and 10  $\mu\text{m}$  (right, (c) and (d)).

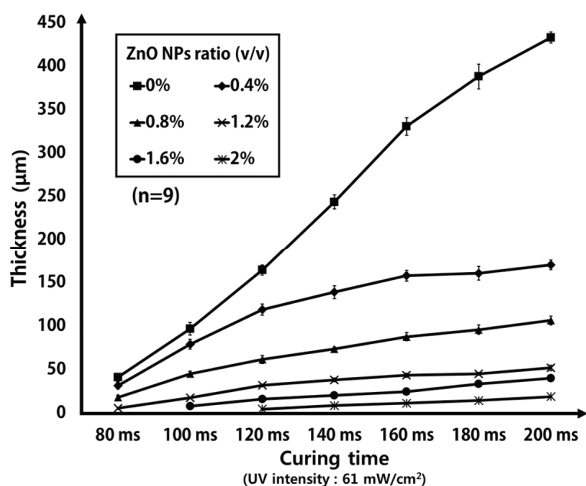


**Figure 4.** Comparison of fabricated micropattern thickness between the PEGDA solution and PEGDA solution mixed with ZnO NPs for absorbing ray energy from a UV light source. The gradient of the curve of the photocurable solution without ZnO NPs is dramatically steeper than that of the mixed photoresin with the particles. The results mean that it is practicable to appropriately adjust the layer thickness of generated micropatterns to be insensitive and uniform against the curing time of a light source.

droxy-2-methylpropiophenone photoinitiator (Irgacure 1173, Sigma-Aldrich) was flowed into the microfluidic channel. After being completely fabricated, the microobjects could be gathered by injecting and passing rinsing solution in the channel.

To compare the smooth degree, two pyramid-like microstructures were created using an equal three-dimensional CAD file with different layer thicknesses cut out as shown in Figure 3(a) and (b). The first rough structure is made up of five layers and the thickness of each layer is 34  $\mu\text{m}$ , and the second exquisite object consists of 51 layers stacked at a thickness of 3.4  $\mu\text{m}$ . When viewed through an optical microscope, the boundaries of the layer were clearly visible in the thick-layer microparticle, but the boundaries were not observed in the thin-layer microparticle. This aspect was also clearly confirmed by a scanning electron microscope (SEM), and the results were the same as that seen by the optical microscope.

Although a structure having a low gradient can be created as shown in Figure 3(b), to fabricate delicate structures in which the slope is steep or varies depending on the position is also possible. Thus, fairly sophisticated three-dimensional microstructures, consisting of thin layers of 3.4  $\mu\text{m}$ , can be created by converting various 3D drawing files such as the microneedle and microlens patterns shown in Figure 3(c) and (d).

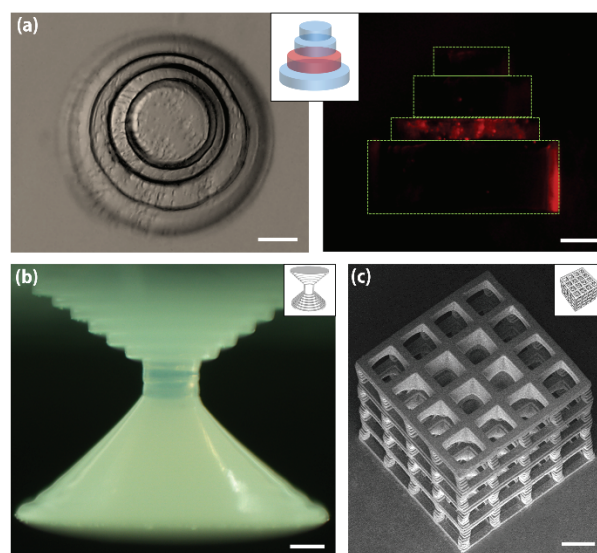


**Figure 5.** Fabricated three-dimensional multimaterial microstructure and three-dimensional microstructures. (a) A four-layered pagoda microstructure composed of non-fluorescent (1st, 2nd, and 4th layer) photopolymers, polyethylene glycol diacrylate, and fluorescent (3rd layer) microparticles with a photoresin. The left and right images are top and lateral view, respectively, of the layered microstructure observed by an optical and a fluorescent microscope. (b) A circular-shape table microstructure imaged using an optical microscope with weak light, and (c) A 4 $\times$ 4 $\times$ 4 microstructure observed by SEM. The microstructures shown in (b) and (c) were fabricated using a ZnO NP mixed photocurable polymer and the inset images are 3D drawing design (CAD) files. (Scale bar: (a) and (b) is 100  $\mu\text{m}$ , and (c) 200  $\mu\text{m}$ ).

### Use of UV-Absorbable Nanoparticles to Create a Thin Layer

In order to fabricate 3D microstructures through elaborately-sliced floor maps from three-dimensional CAD files, a printing technique capable of realizing such precision would be required. By the square-type micromirrors in size of 14  $\mu\text{m}$  and 4 $\times$  magnification objective lens used in the photolithography equipment, the resolution on the XY axis could be fairly and precisely adjusted to 3.5  $\mu\text{m}$ . Accordingly, the resolution control on the Z-axis must be coordinated not only with the stepper motor but also with the photocurable polymer to fabricate delicate three-dimensional structures. For example, in a three-dimensional hollow structure, a number of holes must exist in all XYZ positions, which will only be realized in an elaborate three-dimensional printing technique. In this experiment, because the difference in thickness produced at slight energy adjustments in the PEGDA solution dramatically changed, as shown in Figure 4, it has been difficult to fabricate thin and uniform layers.

Since the light source used in this system is an ultraviolet (UV) ray of 365-nm wavelength, it would be possible to control the layer thickness of the produced micropatterns by mixing special materials capable of absorbing this projected light energy well. In order for the solution mixture to obtain an excellent ability to absorb the UV light energy, a variety of materials that can absorb the energy of ultraviolet wavelength bands should be mixed in the solution; many studies have been done on this by using zinc oxide nanoparticle (ZnO NP)<sup>33–35</sup>, a UV-absorbable material. The ZnO NP with UV blocking properties is one of biocompatible materials and is being actively applied to biomedical fields<sup>36,37</sup>. In addition, because it maintains transparency<sup>38,39</sup> in a mixture with a small amount added, it can minimize the opaqueness on the existing photocurable polymers that remain transparent. Therefore, when fabricated by mixing a small amount of ZnO NP, thin layers can be formed while maintaining transparency, and structures applicable to the biomedical field can be created. In this study, we mixed zinc oxide nanoparticle dispersion with various volume proportions from 0 to 2% in the resin mixed with PEGDA and photoinitiator solution at a volume ratio of 10 to 1. After mixing the ZnO NPs, the layer thickness of the produced micropatterns was several micrometers thin and insensitive to change in light curing time as shown in Figure 4, and, therefore, even though sometimes an error occurs in the system's output, a thin and uniform layer thickness of approximately 3.4  $\mu\text{m}$  can be created in case of 2% ZnO NP mixed solution with 120 ms curing time.

### Elaborate 3D Hydrogel Structures Using a Multimaterial

Due to the use of microfluidic channels capable of transporting multiple fluids simultaneously or separately, we can pass different kinds of solutions into a single channel. Thus, using the feature of the microfluidic channel, a three-dimensional microstructure made up of two or more materials can be fabricated, and, in addition, the structure can be detached from the channel using washing flow as shown in Figure 5(a). The first two layers and the last layer were produced by the non-fluorescent PEGDA solution, and the third layer was made of a mixed solution with the PEGDA prepolymer and red fluorescent microparticles (Fluorescent Nile Red Particles, excitation: 514 nm and emission: 557 nm, 1.7–2.2  $\mu\text{m}$ , Spherotech). To make sure that the layered microstructure was properly created, it was collected by washing the channel using ethanol (99%, Daejung) and laid on the side and

observed through a fluorescent lamp apparatus (U-HGLGPS, Olympus).

It was confirmed that the sophisticated layer thickness can be generated by mixing materials which can absorb the light source wavelength band used in this system (Figure 4), and complete three-dimensional microstructures were thus fabricated. In order to create three-dimensional microstructures, 3D drawing design files were converted and loaded to the DMD of the system (top-right of Figure 5(b) and (c)), and we could generate the elaborate microstructures (Figure 5(b) and (c)). The circular table-shaped microparticles (Figure 5(b)) collected from the washing process were laid on the side and imaged under an optical microscope (IX, DP73, Olympus) under weak light. To demonstrate the successful fabrication of a complex three-dimensional microstructure, we also created 4×4×4 microscaffold using the system with the resin and observed it using SEM as shown in Figure 5(c).

### Conclusion

We demonstrated a micro three-dimensional printing system by combining the OFML system that can fabricate various two-dimensional polymeric micropatterns using a dynamic micromirror to project light and a single-axis stepper motor to control the layer height of the microfluidic channel inside. Although it would be desirable to create all three-dimensional microstructures using only a single type of microfluidic channel, in order to minimize the amount of solution used, we simulated the optimal microfluidic channel design according to the height of the microstructure to be fabricated. By adjusting the layer thickness of the microstructure to be produced, we could fabricate three-dimensional micropatterns and particles holding smooth surfaces with thin layers such as microneedle and lens structures. Also, for biomedical applicability, ZnO NP materials, transparent, biocompatible, and capable of absorbing the wavelength of the light source, were mixed with a photocurable polymer to make the layer thinner and more uniform. As a result, very sophisticated three-dimensional micropatterns and particles could be fabricated, and, in addition, various resins could be transported into the microfluidic channel to create microstructures containing multiple substances.

We expect the micro three-dimensional printing system to help in a variety of research fields and applications including *in situ* synthesis of multimaterial and complicated microstructures in microfluidic de-

vices, hybrid cell culture systems for cell and tissue engineering, and microstructure fabrication systems for complex geometry analysis. We also anticipate that the combination of fabricated intricate 3D microstructures with a photocurable resin can help create suitable large millimeter or centimeter-size structures and experiments.

## Materials and Methods

### Materials

We mixed PEGDA ( $M_n = 700$ , Sigma-Aldrich) with 10% v/v of photoinitiator (2-hydroxy-2-methylpropiophenone, Irgacure 1173, Sigma-Aldrich) to create a photocurable resin. In order to delicately control the layer thickness, ZnO (nanoparticles, <100 nm particle size (DLS), <35 nm average particle size (APS), 50 wt% in H<sub>2</sub>O, dispersion, Sigma-Aldrich) material was used, and the photocurable resin mixed with 2% v/v of the ZnO material. After fabrication, the residual resin and fully created three-dimensional microstructure were washed using ethanol (99%, Daejung) and collected. A fluorescent substance (Fluorescent Nile Red Particles, 1.7–2.2  $\mu\text{m}$ , 1% w/v, Spherotech) was used to observe the microstructure without background color.

### Setup of the 3D Printing System

We used a single-axis stepper motor (LAC10A-T4, Zaber) and an OFML system for micro three-dimensional printing. The OFML system is basically divided into a light source, light reflector, and an optical microscope. A mercury–xenon lamp (L9588, Hamamatsu) was used as a UV light source, and a digital micromirror device (DMD, 1024×768, Texas Instruments) utilized to dynamically control the shape of the light pattern used for polymerizing the photocurable resin. An optical microscope (IX71, Olympus) with 4× magnification objective lens (UPlanFL N, Olympus) and a charge-coupled device camera (DP73, Olympus) are used to fabricate and observe the created non-fluorescent microstructures. Also, in order to observe fluorescent materials, we used a light guide-coupled illumination system (U-HGLGPS, Olympus) with the optical microscope.

### Fabrication of a Microfluidic Channel

The microfluidic channel was created by curing a PDMS (Sylgard 184, Dow Corning) base mixed with a curing agent in a 10:1 ratio on an SU-8 mold and

baking it at 120 °C on a hot plate for 1 h. In order to attach generated micropatterns onto the ceiling of the microfluidic channel, we bonded a circular glass slide to the channel ceiling using air plasma treatment (CUTE-MPR, Femto Science) for 1 min (14 sccm, 500 mTorr, 100 W) after removing the form from the SU-8 mold. After fabrication of the microfluidic channel, the channel was bonded with a PDMS-coated glass slide using a similar air plasma treatment process as that used in the microfluidic channel.

### Flow Control of the Microfluidic Channel

All microfluidic channels were controlled by Microfluidic Flow Control System (MFCS-EZ, FLUIGENT) device. In the case of resin material exchange, the process performed until the resin was completely exchanged under flow rate of 35  $\mu\text{L}/\text{min}$ , and structural detaching process carried out under flow rate of 5 mL/min.

**Acknowledgements** This work was supported by the National Research Foundation of Korea Grant funded by the Korean Government (NRF-2017R1A2B4005933, NRF-2018R1A6A1A03025708).

**Conflict of Interests** The authors declare no competing financial interests.

## References

1. Wise, K.D. & Najafi, K. Microfabrication techniques for integrated sensors and microsystems. *Science* **254**, 1335-1342 (1991).
2. Hierlemann, A., Brand, O., Hagleitner, C. & Baltes, H. Microfabrication techniques for chemical/biosensors. *Proc. IEEE* **91**, 839-863 (2003).
3. Marzencki, M., Ammar, Y. & Basrou, S. Integrated power harvesting system including a MEMS generator and a power management circuit. *Sens. Actuators, A* **145**, 363-370 (2008).
4. Beebe, D.J., Moore, J.S., Yu, Q., Liu, R.H., Kraft, M.L. & Devadoss, C. Microfluidic tectonics: A comprehensive construction platform for microfluidic systems. *Proc. Natl. Acad. Sci. U. S. A.* **97**, 13488-13493 (2000).
5. Anderson, J.R., Chiu, D.T., Jackman, R.J., Chemavskaya, O., McDonald, J.C., Wu, H., Whitesides, S.H. & Whitesides, G.H. Fabrication of topologically complex three-dimensional microfluidic systems in PDMS by rapid prototyping. *Anal. Chem.* **72**, 3158-3164 (2000).
6. Lin, C.-H., Lee, G.-B., Lin, Y.-H. & Chang, G.-L. A

- fast prototyping process for fabrication of microfluidic systems on soda-lime glass. *J. Micromech. Microeng.* **11**, 726-732 (2001).
7. Hnatovsky, C., Taylor, R.S., Simova, E., Bhardwaj, V.R., Rayner, D.M. & Corkim, P.B. Polarization-selective etching in femtosecond laser-assisted microfluidic channel fabrication in fused silica. *Opt. Lett.* **30**, 1867-1869 (2005).
  8. Takeuchi, S., Garstecki, P., Weibel, D.B. & Whitesides, G.M. An axisymmetric flow-focusing microfluidic device. *Adv. Mater.* **17**, 1067-1072 (2005).
  9. Choi, C.H., Jung, J.H., Hwang, T.S. & Leezz, C.S. In situ microfluidic synthesis of monodisperse PEG microspheres. *Macromol. Res.* **17**, 163-167 (2009).
  10. Rhee, M., Valencia, P.M., Rodriguez, M.I., Langer, R., Farokhzad, O.C. & Karnik, R. Synthesis of size-tunable polymeric nanoparticles enabled by 3D hydrodynamic flow focusing in single-layer microchannels. *Adv. Mater.* **23**, H79-H83 (2011).
  11. Chu, L.Y., Utada, A.S., Shah, R.K., Kim, J.W. & Weitz, D.A. Controllable monodisperse multiple emulsions. *Angew. Chem. Int. Ed.* **46**, 8970-8974 (2007).
  12. Adams, L.L.A., Kodger, T.E., Kim, S.H., Shum, H.C., Franke, T. & Weitz, D.A. Single step emulsification for the generation of multi-component double emulsions. *Soft Matter* **8**, 10719-10724 (2012).
  13. Jenness, N.J., Hill, R.T., Hucknall, A., Chilkoti, A. & Clark, R.L. A versatile diffractive maskless lithography for single-shot and serial microfabrication. *Opt. Express* **18**, 11754-11762 (2010).
  14. Bae, H.J., Bae, S., Yoon, J., Park, C., Kim, K., Kwon, S. & Park, W. Self-organization of maze-like structures via guided wrinkling. *Sci. Adv.* **3**, e1700071 (2017).
  15. Han, S., Bae, H.J., Kim, J., Shin, S., Choi, S.E., Lee, S.H., Kwon, S. & Park, W. Lithographically encoded polymer microtaggant using high-capacity and error-correctable QR Code for anti-counterfeiting of drugs. *Adv. Mater.* **24**, 5924-5929 (2012).
  16. Chung, S.E., Park, W., Park, H., Yu, K., Park, N. & Kwon, S. Optofluidic maskless lithography system for real-time synthesis of photopolymerized microstructures in microfluidic channels. *Appl. Phys. Lett.* **91**, 041106 (2007).
  17. Chung, S.E., Park, W., Shin, S., Lee, S.A. & Kwon, S. Guided and fluidic self-assembly of microstructures using railed microfluidic channels. *Nat. Mater.* **7**, 581-587 (2008).
  18. Lee, H., Kim, J., Kim, H., Kim, J. & Kwon, S. Colour-barcoded magnetic microparticles for multiplexed bioassays. *Nat. Mater.* **9**, 745-749 (2010).
  19. Park, W., Han, S., Lee, H. & Kwon, S. Free-floating amphiphilic picoliter droplet carriers for multiplexed liquid loading in a microfluidic channel. *Microfluid. Nanofluid.* **13**, 511-518 (2012).
  20. Yoon, J., Kim, K. & Park, W. Modulated grayscale UV pattern for uniform photopolymerization based on a digital micromirror device system. *Appl. Phys. Lett.* **111**, 033505 (2017).
  21. Nam, S.M., Kim, K., Kang, I.S., Park, W. & Lee, W. Generation of 3D microparticles in microchannels with non-rectangular cross sections. *BioChip J.* **13**, 226-235 (2019).
  22. Kim, L.N., Choi, S.-E., Kim, J., Kim, H. & Kwon, S. Single exposure fabrication and manipulation of 3D hydrogel cell microcarriers. *Lab Chip* **11**, 48-51 (2011).
  23. Song, S.-H., Kim, K., Choi, S.-E., Han, S., Lee, H.S., Kwon, S. & Park, W. Fine-tuned grayscale optofluidic maskless lithography for three-dimensional freeform shape microstructure fabrication. *Opt. Lett.* **39**, 5162-5165 (2014).
  24. Habasaki, S., Lee, W.C., Yoshida, S. & Takeuchi, S. Vertical flow lithography for fabrication of 3D anisotropic particles. *Small* **11**, 6391-6396 (2015).
  25. Shim, T.S., Yang, S.M. & Kim, S.H. Dynamic designing of microstructures by chemical gradient-mediated growth. *Nat. Commun.* **6**, 6584 (2015).
  26. Arai, K., Iwanaga, S., Toda, H., Genci, C., Nishiyama, Y. & Nakamura, M. Three-dimensional inkjet biofabrication based on designed images. *Biofabrication* **3**, 034113 (2011).
  27. Xu, T., Zhao, W., Zhu, J.M., Albanna, M.Z., Yoo, J.J. & Atala, A. Complex heterogeneous tissue constructs containing multiple cell types prepared by inkjet printing technology. *Biomaterials* **34**, 130-139 (2013).
  28. Hardin, J.O., Ober, T.J., Valentine, A.D. & Lewis, J.A. Microfluidic printheads for multimaterial 3D printing of viscoelastic inks. *Adv. Mater.* **27**, 3279-3284 (2015).
  29. Tayalia, P., Mendonca, C.R., Baldacchini, T., Mooney, D.J. & Mazur, E. 3D cell-migration studies using two-photon engineered polymer scaffolds. *Adv. Mater.* **20**, 4494-4498 (2008).
  30. Koroleva, A., Gill, A.A., Ortega, I., Haycock, J.W., Schlie, S., Gittard, S.D., Chichkov, B.N. & Claeysens, F. Two-photon polymerization-generated and micromolding-replicated 3D scaffolds for peripheral neural tissue engineering applications. *Biofabrication* **4**, 025005 (2012).
  31. Shaw, L.A., Chizari, S., Shusteff, M., Naghsh-Nilchi, H., Di Carlo, D. & Hopkins, J.B. Scanning two-photon continuous flow lithography for synthesis of high-resolution 3D microparticles. *Opt. Express* **26**, 13543-13548 (2018).
  32. Lölsberg, J., Cinar, A., Felder, D., Linz, G., Djeljadini, S. & Wessling, M. Two-photon vertical-flow lithography for microtube synthesis. *Small* **15**, 1901356 (2019).



33. Shanshool, H.M., Yahaya, M., Yunus, W.M.M. & Abdullah, I.Y. Polymer-ZnO nanocomposites foils and thin films for UV protection. *AIP Conf. Proc.* **1614**, 136-141 (2014).
34. Goh, E.G., Xu, X., McCormick, P.G. Effect of particle size on the UV absorbance of zinc oxide nanoparticles. *Scr. Mater.* **78**, 49-52 (2014).
35. Kim, D.H. & Sung, A.Y. Physical properties and ophthalmic application of high functional materials with zinc oxide and titanium oxide nanoparticles. *J. Nanosci. Nanotechnol.* **16**, 11035-11039 (2016).
36. Mirzaei, H. & Darroudi, M. Zinc oxide nanoparticles: Biological synthesis and biomedical applications. *Ceram. Int.* **43**, 907-914 (2017).
37. Nain, V., Kaur, M., Sandhu, K.S., Thory, R. & Sinhar, A. Development, characterization, and biocompatibility of zinc oxide coupled starch nanocomposites from different botanical sources. *Int. J. Biol. Macromol.* **162**, 24-30 (2020).
38. Shrestha, M. & Lau, G.-K. Tunable window device based on micro-wrinkling of nanometric zinc-oxide thin film on elastomer. *Opt. Lett.* **41**, 4433-4436 (2016).
39. Olson, E., Li, Y., Lin, F.Y., Miller, A., Liu, F., Tsyrenova, A., Palm, D., Curtzwiler, G.W., Vorst, K. L., Cochran, E. & Jian, S. Thin biobased transparent UV-blocking coating enabled by nanoparticle self-assembly. *ACS Appl. Mater. Interfaces* **11**, 24552-24559 (2019).